

## An optically detected cyclotron resonance study of bulk GaAs

This content has been downloaded from IOPscience. Please scroll down to see the full text.

1994 Semicond. Sci. Technol. 9 198

(<http://iopscience.iop.org/0268-1242/9/2/012>)

View [the table of contents for this issue](#), or go to the [journal homepage](#) for more

Download details:

IP Address: 131.152.34.219

This content was downloaded on 18/05/2014 at 16:37

Please note that [terms and conditions apply](#).

# An optically detected cyclotron resonance study of bulk GaAs

J G Michels†, R J Warburton†, R J Nicholas† and C R Stanley‡

† Clarendon Laboratory, Parks Road, Oxford OX1 3PU, UK

‡ Department of Electronics and Electrical Engineering, University of Glasgow, Glasgow G12 8QQ, UK

Received 29 October 1993, accepted for publication 29 November 1993

**Abstract.** We have measured optically detected cyclotron resonance using far-infrared radiation on an exceptionally pure sample of GaAs in fields up to 15.5 T. This relatively new experimental technique is shown to offer high resolution of free and donor impurity-bound electron transitions without the reproducibility problems of photoconductivity. The data confirm the existence of metastable donor states and provide a detailed picture of chemical shifts. The optically detected cyclotron resonance signal represents an interaction between the donor bound electron states which are influenced by the far-infrared radiation and the donor bound exciton states which are responsible for the photoluminescence. Attenuation of the luminescence intensity under far-infrared illumination is primarily the result of a *photothermal effect*. At high fields, there is indication of an interaction between the electron and excitonic energy levels.

## 1. Introduction

Far-infrared (FIR) magnetospectroscopy employing transmission and absorption measurements has been extensively used to study band structure and shallow donor states in semiconductors. The change in electrical conductivity with FIR illumination has also been employed to detect transitions between the shallow donor levels. In these photoconductivity experiments, an increase in electrical conductivity occurs when the FIR excites a bound donor electron to a higher state, thereby increasing its probability of being promoted into the conduction band.

Optically detected cyclotron resonance (ODCR) differs from other forms of magnetospectroscopy in that the intensity of luminescence excited by a visible laser is monitored rather than the direct absorption of far-infrared (FIR) radiation. ODCR is a potentially valuable tool in the study of semiconductor materials for several reasons. Firstly, experiments on undoped samples are possible because the optical pumping of the visible laser provides the necessary carriers. Secondly, photomultiplier tubes used to detect luminescence offer far more sensitivity than their counterpart microwave or FIR detectors, and finally, the possibility now exists for a simultaneous study of electrons and holes.

The feasibility of ODCR at microwave frequencies was first demonstrated by Romestain and Weisbuch, who used the method for determining band masses in CdTe and GaAs [1]. Extension of the resonant frequencies to the far-infrared has been shown to provide an enhancement in the resolution and sensitivity

of the technique [2–4]. Recently we have used ODCR to determine the conduction band effective mass and quantify offset effects in undoped GaAs/AlGaAs quantum well structures [5] and to study superlattice orbits and impurity states in InGaAs/GaAs [6].

In this paper, a high purity sample of n-type GaAs is studied using FIR-induced ODCR. Extremely good resolution of the system enabled observation of the cyclotron resonance, with a spin-split peak discernible above 4.3 T, and a complete range of bound and metastable impurity transitions. Chemical shifts due to the presence of different donor species are clearly resolved. Comment is offered on an anomaly in the ODCR signal at high fields. A critical factor in the experimental success of ODCR is seen to be the magnitude of the ODCR signal, which reflected up to a 50% modulation of the PL intensity.

## 2. Theory

With the application of a magnetic field, energy levels of free carriers in a semiconductor are quantized into Landau levels (LL) separated by  $\hbar\omega_c$ . Below each LL exists an additional series of states due to carriers bound to impurities in the sample. Observed experimental transition energies of these impurity states are in good agreement with numerical solutions of the Schrödinger equation for a single electron under the simultaneous action of a static Coulomb potential and uniform magnetic field. Prominent among these studies is that

of Makado and McGill [7], who calculated the energy eigenvalues of such a hydrogen-like system in a large magnetic field for the complete spectrum of bound states. These values have been successfully used to identify the origin of experimentally observed transitions for several photoexcitation and transmission spectra [8–12].

Further refinement in the calculation of energy levels was offered by Simola and Virtamo [12], who considered the solution of the Schrödinger equation in the high-field limit and found that a series of so-called metastable states exist in the continuum below each Landau level. Unlike bound states, the metastable states have no zero-field analogue and consequently cannot be labelled using hydrogen spectrum notation.

The characterization of impurity states can be confusing because it employs different labelling systems for the weak ( $\gamma \leq 1$ ), intermediate ( $\gamma \sim 1$ ) and high-field ( $\gamma \geq 1$ ) regions, with

$$\gamma = \frac{1}{2} \frac{\hbar \omega_c}{R_y^*}$$

where  $R_y^*$  is the effective Rydberg or binding energy of the impurity, and  $\omega_c = eB/m^*$  is the cyclotron frequency.  $\gamma$  is then a dimensionless parameter, being the ratio of the zero-point cyclotron energy to the effective Rydberg. The situation has become somewhat muddled as various authors have labelled high-field states with their corresponding low-field label, a correspondence that further theoretical work has shown does not exist [10, 13].

In weak fields, the energy eigenvalues are characterized by the Zeeman splitting nomenclature and atomic numbers ( $n, l, m$ ). In the high-field limit, states may be assigned quantum numbers ( $N, m, \nu$ ) where  $N$  denotes the Landau level from which the state is derived,  $m$  ( $= N, N - 1, \dots, -\infty$ ) is the magnetic quantum number, and  $\nu$  ( $= 0, 1, \dots, \infty$ ) equals the number of nodes of the eigenstate in the direction of the magnetic field. The parity of the eigenstate is given by  $\pi = (-1)^{m+\nu}$ .  $m$  and  $\pi$  remain good quantum numbers throughout the field spectrum. Also applying to the entire field range are the electric dipole selection rule,  $\Delta m = \pm 1$  for a Faraday configuration, and the parity restriction  $\pi_i \pi_f = -1$ , where  $\pi_i$  and  $\pi_f$  are the parities of the initial and final states respectively.

No quantitative theoretical information existed concerning the metastable states until recently, when  $E_{N,m,\nu} - E_{N-m,-m,\nu}$ , the energy difference between states ( $N, m, \nu$ ) and ( $N - m, -m, \nu$ ), was shown experimentally to be  $m\hbar\omega_c$  [9]. Optical  $\Delta m = \pm 1$  transitions thus yield pairs of lines separated by  $\omega_c$  in frequency. von Klarenbosch *et al* [8] used this to label many experimentally observed low-field transitions with energy above the  $N = 0$  LL as metastable states. We employ the energy level calculations of Makado and McGill and the experimental results of von Klarenbosch *et al* to classify our observed bound and metastable impurity transitions.

### 3. Experimental set-up

ODCR requires two light sources: one in the visible to excite the luminescence and one in the far-infrared or microwave region. Photoluminescence (PL) was excited with a 3 mW solid state laser diode operating at 670 nm, used for its greater amplitude stability than conventional HeNe lasers. A CO<sub>2</sub>-pumped molecular gas laser provided the FIR radiation in a series of lines from 47–570  $\mu\text{m}$ . This was directed through a highly polished brass waveguide and series of mirrors onto the sample substrate, mounted in a Faraday configuration at the field centre of an 18 T superconducting magnet. The 670 nm radiation arrived at the sample by means of one arm of a bifurcated optical bundle; the second arm collected the luminescence and returned it to a 0.5 m spectrometer, where the intensity was measured with a GaAs photomultiplier tube. The laser diode provided a power density at the sample of  $\sim 4 \text{ mW cm}^{-2}$ . The sample of GaAs has a transport-measured peak mobility  $\mu \sim 402\,000 \text{ cm}^2 \text{ V}^{-1} \text{ s}^{-1}$ , carrier concentration ( $N_D - N_A$ ) of  $2.8 \times 10^{13} \text{ cm}^{-3}$  and is described in detail in [14]. Luminescence spectra will be presented in section 5 as part of the discussion relating to ODCR mechanisms.

Three types of data were collected: (1) photoluminescence (PL) measurements, (2) ODCR and (3) infrared modulated photoluminescence or IMPL. IMPL involves measuring the ODCR signal as a function of PL wavelength with the FIR allowed to illuminate the sample and the magnetic field fixed to correspond to a resonance position. The IMPL would then be compared with a PL spectrum taken at the same field value to determine how the FIR radiation impacted on the differing PL transitions. For PL and IMPL measurements, the spectrometer slits were narrowed in order to resolve the principal triad of peaks in the PL spectrum, while ODCR work

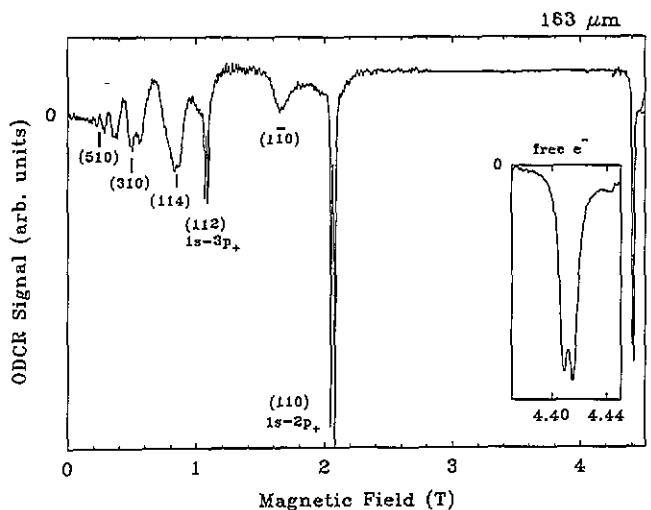


**Figure 1.** ODCR signal for a FIR wavelength of 163  $\mu\text{m}$ . Transitions with hydrogen-like analogues are sharply defined (i.e.  $1s-2p_+$ ,  $3p_+$ ). The splitting is due to central cell effects of different impurities. Low-field, higher energy metastable transitions show broad profiles (310, 510 etc). The free-electron transition is at 4.41 T with enough resolution to show a spin-split peak.

was performed with the slits set wide enough to take in all three without distinguishing between them (approximately 0.5 cm). In this way, luminescence intensity was maximized for ODCR traces and the system resolution was comparable to the diamagnetic shift of the luminescence peak, making it unnecessary to continually adjust the detection wavelength when sweeping the field.

The laser diode beam was chopped to provide a reference signal for a lock-in amplifier in PL measurements. ODCR and IMPL involved the additional step of taking output from the lock-in amplifier connected to the luminescence signal and feeding it into a second lock-in whose reference was provided by chopping the CO<sub>2</sub> laser beam. This configuration maximized the ODCR signal-to-noise ratio and ensured that effects seen were not spurious in origin. The PL signal was chopped at ~ 2 kHz and the FIR signal at ~ 20 Hz. All ODCR data were taken with the sample at ~ 2.2 K. Figure 1 is a representative ODCR trace for a FIR wavelength of 163 μm, showing the wealth of impurity transitions and a spin-split cyclotron resonance at 4.41 T.

#### 4. Experimental results

##### 4.1. Free-electron cyclotron resonance

Free-electron cyclotron resonance energies for the 18 different FIR frequencies used are collected together in

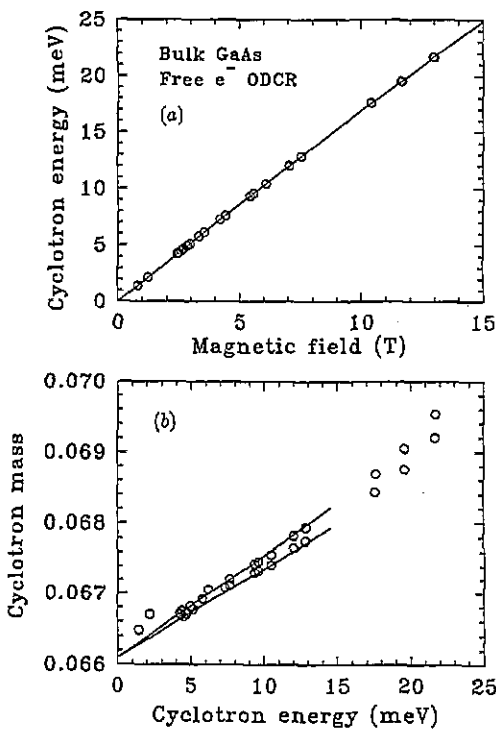


Figure 2. (a) Free-electron cyclotron resonance energies as a function of field. The slightly nonlinear slope is a consequence of polaron coupling and non-parabolic band structure. (b) Experimentally determined electron effective mass. The lines show a linear fit at low energies to determine the value(s) of  $K_2$  (cf text and [15]).

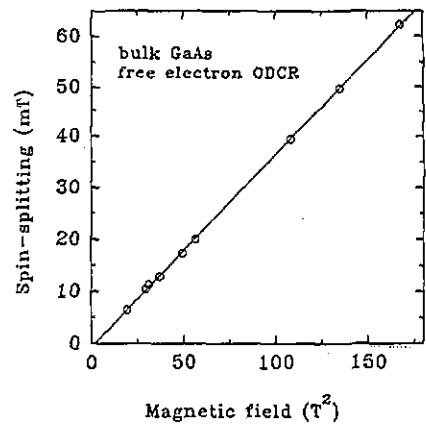


Figure 3. The splitting between the spin-(+) and spin-(-) free-electron transitions follows a characteristic  $B^2$  dependence [16].

figure 2(a), a plot of the cyclotron energy,  $E_{CR} = \hbar e B / m^*$ , against resonant field position,  $B$ , where  $m^*$  is the carrier effective mass. The data points lie on a curve resulting from the combined effect of polaron coupling and the band structure. Figure 2(b) shows the cyclotron mass,  $m^*$ , as a function of energy. Extrapolated to  $B = 0$ , the data give an effective mass of  $m_0^* = (0.0661 \pm 0.0001)m_0$ , which agrees well with a previous cyclotron resonance study of bulk GaAs by Hopkins *et al* [15]. These authors fitted the effective mass at low  $E_{CR}$  to

$$m^* = m_0^* \left( 1 - \frac{2K_2}{E_g} E_{CR} \right)$$

with  $E_g$  the bandgap and  $K_2$  determined empirically from the slope of the energy-mass relationship. Our data indicate  $K_2$  values of  $-1.67$  and  $-1.45$ , for the spin-up and spin-down transitions, slightly lower than the data of Hopkins *et al*.

Generally, spin-splitting of the Landau levels is the result of the Zeeman interaction, but only manifests itself in cyclotron resonance measurements because of the energy dependence of the  $g$ -factor, which changes the magnitude of the splitting for successive Landau levels. This effect becomes visible in our data at fields above 4.4 T. Following the work of Sigg *et al* [16] on the field dependence of splitting in GaAs, the magnitude of the spin-splitting is plotted against  $B^2$  and shows excellent agreement with their result based on a five-band  $k \cdot p$  model (figure 3).

##### 4.2. Lower energy impurity transitions and central cell effects

In addition to the free-electron cyclotron resonance, a full range of transitions was observed from the ground to excited states of shallow donor impurities present in the sample. In describing these transitions it is convenient to split them into two groups: those with low-field bound hydrogen-like analogues and those without, the latter being the previously mentioned metastable states. Experimentally, those transitions with hydrogen-like analogues appeared as sharp resonances, with a

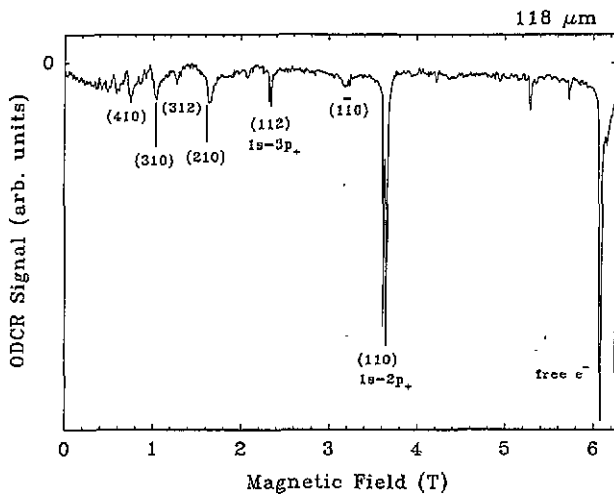


**Figure 4.** ODCR signal for a FIR wavelength of 118  $\mu\text{m}$ . Differences in hydrogen-like and metastable state signatures are apparent (cf figure 1).

hyperfine separation caused by central cell effects of the different impurities present in the sample, while metastable states had broad resonance profiles (figure 4).

The experimental transition energies from the 1s ground state to the hydrogen-like states up to and including the  $3p_+$  energy level were found to match the theoretical results of Makado and McGill through the intermediate field region. An effective Rydberg  $R_y^*$  of 5.72 meV was used in the calculations. The

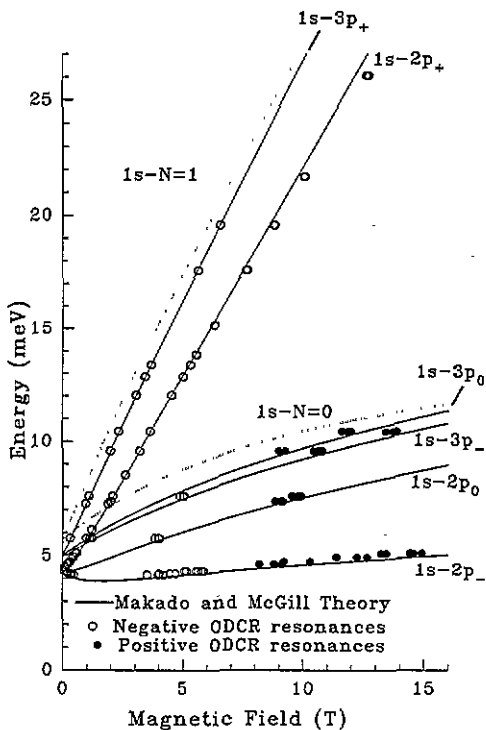


**Figure 5.** Transitions with hydrogen-like state analogues are fitted to the theory of Makado and McGill, which calculates the energy spectrum of a hydrogen atom in a large magnetic field. An effective Rydberg of 5.72 meV was used in the calculation. Central cell shifts of different impurities are resolved as repeating groups of triplets, especially on the flatter lower energy transitions. Also shown are the predicted energy levels of the  $1s-N = 0, 1$  Landau level transitions.

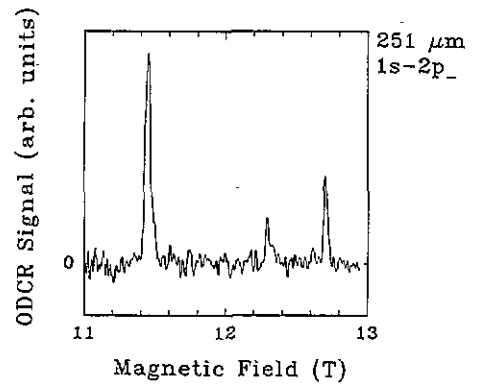


**Figure 6.**  $1s-2p_-$  transition for 251  $\mu\text{m}$ . The flat slope of the transition at high fields results in chemical shifts due to S, Sn/Se and Si donors being spread over 1.5 T.

energy of these resonances is plotted as a function of field in figure 5, with the full curves representing the energy spectrum determined by the analysis of Makado and McGill. The slight discrepancy between theory and experiment at high fields is caused by band non-parabolicity, which was not considered by Makado and McGill.

The large number of incident frequencies coupled with high resolution of the ODCR technique provide a detailed picture of the central cell effects in this GaAs sample. Previous studies [17, 18] employed pressure to increase the resolution on transitions with steeper gradients and also used the lower energy transitions  $1s-2p_-$ ,  $1s-2p_0$ ,  $1s-3p_-$  and  $1s-3p_0$ , whose flatter slopes served the same function. In our most extreme case, the small change in energy with increasing field on the  $1s-2p_-$  transition resulted in a 1.5 T wide split of the three chemically shifted resonances (figure 6).

Pictured in figure 7 is the  $1s-3p_+$  transition with a laser wavelength of 163  $\mu\text{m}$ . The three peaks are due to S, Sn/Se and Si donors present in the sample [14]. The lines are narrower than photoconductivity

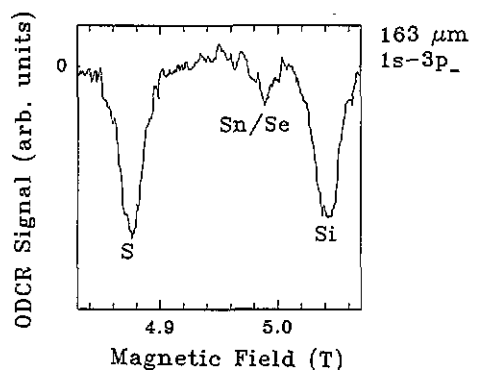


**Figure 7.**  $1s-3p_+$  transition for 163  $\mu\text{m}$ . Even for transitions with much steeper gradients of energy versus field, the high resolution of the odcR technique enabled observation of central cell effects. The discrepancy in linewidth between figures 6 and 7 is due to the larger extent in real space of the  $3p_+$  wavefunction relative to the  $2p_-$  state. Figure 6 represents a positive odcR signal and figure 7 a negative odcR signal (cf section 5).

spectra obtained previously from high mobility MBE-grown n-GaAs, an indication of the purity and highest ever recorded peak mobility of this sample.

### 4.3. Higher energy transitions

In addition to lower energy transitions of the bound hydrogen-like states, we also observed shallow donor transitions to metastable states (*cf* figures 1 and 4). The hyperfine separation of peaks due to central cell corrections of different donors is absent because the energy levels of the final metastable states are considerably broader than the hydrogen-like bound states. ODCR spectra of these low-field features are equivalent to or better than photoconductivity traces taken with the same sample or ones of comparable quality [8, 10]. More importantly, the troublesome adjustment of sample voltage bias is eliminated with ODCR.

In figure 8 the experimentally observed transitions to final states above the  $1s-3p_+$  impurity level are given. The full curves are taken from the photoconductivity study of von Klarenbosch *et al* [8], which labels energy levels following the analysis of Simola and Virtamo [12]. No (200) or (220) metastable states were seen. This is consistent with the hypothesis of von Klarenbosch *et al* [8] that above-bandgap radiation decreases the number of ionized impurities and thereby minimizes the mixing of electron states (210) and (210) responsible for the formation of the (200) and (220) states. von Klarenbosch *et al* [8] use bandgap radiation as an additional check on the identification of transitions. In our case, above-bandgap radiation is inherent in the ODCR system to excite the PL.

For FIR wavelengths of 70 and 118  $\mu\text{m}$ , a high-field tail to the free-electron cyclotron resonance peak was seen (figure 9). These have been observed previously in both ODCR [2, 3] and photoconductivity spectra [19] taken with strong incident FIR power and temperatures above 4 K. Following the analysis of Hawksworth *et al* [19], it is reasonable to assign these resonances

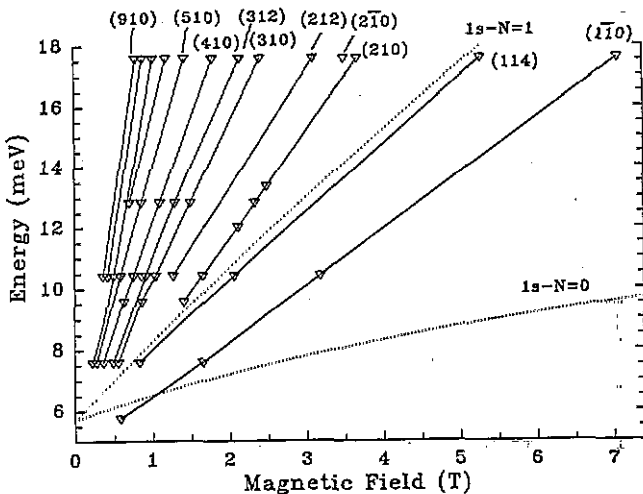


Figure 8. Transitions to states lying above the  $1s-3p_+$  impurity level. Full curves are fits following the analysis of Simola and Virtamo [12].

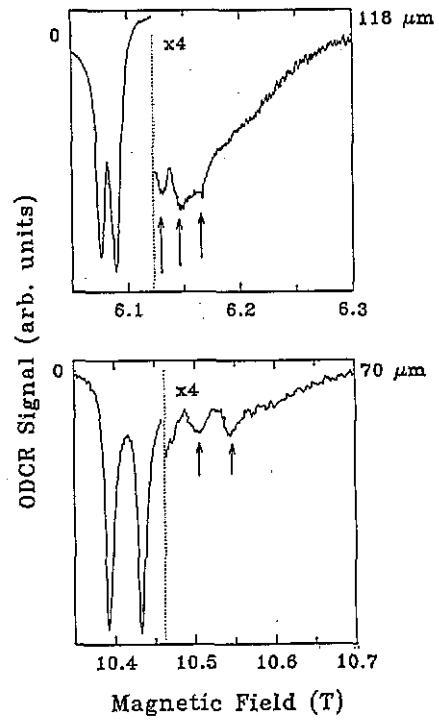


Figure 9. Transitions to metastable states from the  $N = 0$  Landau level are visible in the tail of the free-electron resonance for FIR wavelengths of 118 and 70  $\mu\text{m}$ .

as transitions from the  $N = 0$  Landau level to metastable states. The broad shape is characteristic of a metastable transition, and ODCR spectra match the photoconductivity trace, despite our colder base temperature which limited observation of such states in the Hawksworth experiment.

Despite the large magnitude of the  $1s-2p_{\pm}$  impurity resonances, no transitions involving the  $D^-$  state were observed. The  $D^-$  is the analogue of  $H^-$ ; for GaAs it has an effective Rydberg 5.5% of the Rydberg for the neutral donor.  $D^- - N = 0$  LL transitions have been reported by Grimes *et al*, among others, in recent photoconductivity studies as lying lower in field than the cyclotron resonance transition ([20] and references therein). The lack of  $D^-$  states probably results from neutralization of ionized donors by the visible laser radiation.

### 5. Mechanisms underlying ODCR

There are two distinct processes taking place simultaneously in an ODCR experiment: PL produced by the above-bandgap radiation and absorption of the incident FIR radiation as in a standard CR experiment. The FIR radiation, from 4–25 meV, results in donor-bound electrons being excited to higher energy levels. Detection of these transitions occurs through changes in the PL intensity, which involves recombination of excitons bound to donor/acceptor sites at energies of  $\sim 1.5$  eV. It is worth noting that all the observed resonances with the FIR energy were free or donor-bound single electron transitions rather than transitions within an excitonic complex. This is perhaps not surprising because the number of excitons

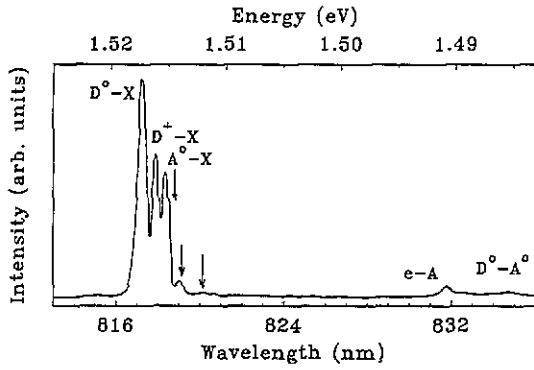


**Figure 10.** The PL spectrum of bulk GaAs taken at  $B = 0$ . The three arrows mark different rotational states of transitions involving excitons bound to neutral acceptors.

created by the visible laser illumination is far fewer than the number of residual impurity electrons†.

Since detection of the electron resonances is inextricably linked to the luminescence, it is necessary first to try to provide a qualitative description of the luminescence mechanism in bulk GaAs. PL measurements were taken over a range of magnetic fields and temperatures to aid in this process. Figure 10 shows the zero-field, 2.2 K PL spectra with the different transitions labelled. Peaks due to the radiative dissociation of excitons bound to neutral and ionized donors and acceptors—( $D^0, X$ ), ( $D^+, X$ ) and ( $A^0, X$ )—respectively, are prominent. Less intense are peaks due to free exciton recombination ( $X$ ) and the free electron–neutral acceptor ( $e, A^0$ )/neutral donor–acceptor ( $D^0, A^0$ ) complex at longer wavelengths [14, 21]. The ( $D^+, X$ ) complex is often represented as ( $D^0, h$ ), a hole binding to a neutral donor, which is an excited state representation of the ( $D^+, X$ ) system.

A study by Bimberg *et al* [22] on the kinetics of recombination in GaAs indicates that excitonic creation is extremely rapid and essentially instantaneous on the scale of bound excitonic lifetimes. Time-resolved luminescence studies show prominent free exciton and ( $D^0, X$ ) peaks after pulses as short as 2 ns. Striking enhancement of donor-related photoluminescence has also been observed when the excitation energy lies just below the bandgap, consistent with excitation of the free excitons [23]. Exciton capture then represents the dominant mechanism for ( $D^0, X$ ) creation [24]. Formation of neutral acceptor complexes, however, is determined by the initial capture of holes by ionized acceptors,  $A^- + h^+ \rightarrow A^0$ , resulting in the neutral acceptor state to which the exciton then binds. This capture of minority charge carriers by ionized impurities is relatively slow when compared with formation of donor bound excitons.

The relative probability of binding to an ionized impurity depends on the effective mass ratio of electrons

† 3 mW of diode illumination provides a power density of  $4.2 \text{ mW cm}^{-2}$ , assuming a factor of ten loss in coupling to the fibre. This results in  $1.42 \times 10^{16} \text{ photons s}^{-1} \text{ cm}^{-2}$ . Assuming a penetration depth of  $5 \mu\text{m}$  and a lifetime of 100 ns, this results in a steady state exciton population of  $\sim 3 \times 10^{12} \text{ cm}^{-3}$ .

and holes,  $\sigma = m_e^*/m_h^*$ ; if  $\sigma < 0.38$  stable binding to ionized donors, ( $D^+, X$ ), occurs [25]. GaAs meets this requirement with  $m_e^* \ll m_h^*$  but the hole is considered to be very weakly bound. This complex competes with ionized acceptors for capture of holes, which generally disappear quickly due to their large capture cross section [22, 26].

The sample was heated up to  $\sim 20 \text{ K}$  in an attempt to increase emission of the free exciton luminescence. While the relative proportion of free exciton PL was increased, total luminescence intensity was drastically reduced, with the different recombination processes affected unevenly. In the temperature region from 2 to 12 K, a rapid decrease of the intensity of the ( $D^0, X$ ) line with increasing temperature was accompanied by an increase in the free electron–acceptor ( $e, A^0$ ) peak. These results are consistent with an earlier study [27], whose authors attributed differing behaviour of the two transitions to an Auger-like process where ( $D^0, X$ ) non-radiative dissociation results in promotion of the ‘donor’ electron up into the conduction band. Although the dominance of non-radiative processes in direct gap materials like GaAs has since been called into question [28], the temperature data indicate a strong link between the efficiency of ( $D^0, X$ ) formation and the number of free electrons as signified by the strength of the ( $e, A^0$ ) line. Failure to increase the amount of free excitonic recombination and the overall reduced levels of luminescence at higher temperatures led us to take all ODCR spectra at 2.2 K.

An applied magnetic field increases the complexity of luminescence originating from excitons bound to impurities. The problem is similar to that of a single electron subjected to simultaneous Coulomb and magnetic forces discussed earlier, except that the exciton replaces the single carrier orbiting the donor complex. The energy spectrum of bound excitons is similarly quantized, with selection rules governing the allowed transitions. Attempts to model the observed intensities of bound excitonic transitions in magnetic fields have characterized the binding energy between exciton and donor as a combination of existing theories for the  $H^-$  and  $H_2$  hydrogen atom. In the former, the electron orbit will be smaller than the hole orbit and the two electrons can be assumed to pair in the  $1s$  state of the donor, with the ‘excitonic hole’ some distance away; the latter envisions the donor and exciton as two interacting H atoms [29, 30]. Magneto-photoluminescence studies of GaAs have primarily attempted to separate transitions due to the presence of different donors [31] and identify the origin of satellite luminescence spectra [32]. In the present study, the spectrometer slit width was coarse when compared with these high resolution PL experiments. Nonetheless, changes in the spectra with field are attributable to reductions in the efficiency of bound excitonic creation and shifts of the underlying excitonic structure.

Figure 11 shows the effect of increasing field on the intensities of the ( $D^+, X$ ), ( $A^0, X$ ), ( $e-A^0$ ) and ( $D^0-A^0$ ) transitions relative to the ( $D^0, X$ ) intensity. A field

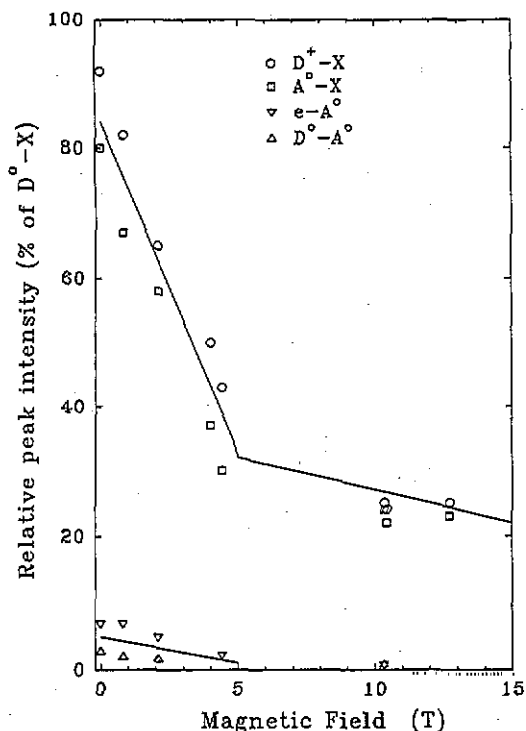


**Figure 11.** An increase in the magnetic field sharply decreases the intensity of the ( $D^+-X$ ), ( $A^0-X$ ), ( $e-A^0$ ) and ( $D^0-A^0$ ) transitions relative to the ( $D^0-X$ ) transition. At fields above 10 T, 70% of the total integrated intensity is a consequence of the ( $D^0-X$ ) transition.

strength of 13 T results in  $\sim 70\%$  of the total integrated PL intensity being due to ( $D^0,X$ ) dissociation, with little contribution from the other lines. The quenching of the ( $D^+,X$ ) transition could be explained by the magnetic field limiting the extent of the donor wavefunction and increasing the binding energy. This would reduce the concentration of  $D^+$  ions by increasing the probability of electron capture to a  $D^0$  state [33]. It is not as clear why the ( $A^0,X$ ) transition diminishes in intensity at these high fields. Spectra taken by Driessen *et al* [32] on high purity GaAs samples show similar intensities of the ( $D^0,X$ ) and ( $A^0,X$ ) peaks at 7 T, although a direct comparison is difficult because of their use of selective line pumping. Formation of the exciton acceptor complex is dependent on the ability of ionized acceptors to capture free holes, which in turn is heavily dependent on the compensation ratio. The relatively low compensation ratio expected for a sample of this quality may explain the discrepancy as most of the available holes would be already bound to donors.

Absorption of the FIR may be viewed as a significant perturbation on this complex luminescence mechanism. ODCR resonances were classed as *negative* if the FIR resulted in a decrease of the PL intensity and *positive* if the PL intensity was increased at resonance. The free-electron, higher energy impurity transitions (i.e.  $m = +1, +2$ , etc) and transitions to metastable states all resulted in negative resonances. Lower energy impurity transitions (i.e.  $m = 0, -1$ ) switched from producing a negative to positive ODCR signal at fields above 8 T. This phenomenon has not been reported in other ODCR

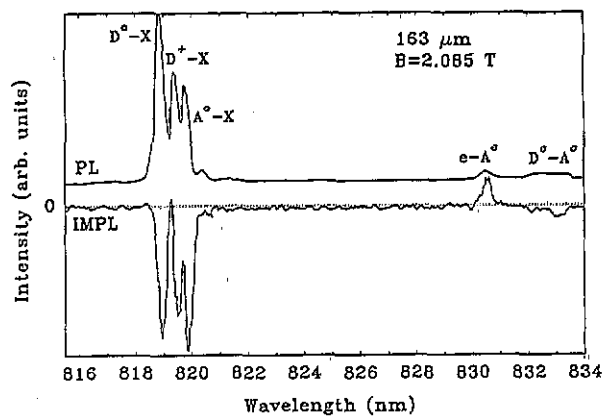


**Figure 12.** PL and IMPL traces for a FIR wavelength of  $163 \mu\text{m}$  taken at 2.085 T, which corresponds to the  $1s-2p_+$  transition. The FIR radiation strongly attenuates the transitions involving bound excitons and the ( $D^0-A^0$ ) complex. An increase in the ( $e-A^0$ ) line indicates a greater number of electrons in the conduction band.

studies. Negative and positive ODCR resonance signals are marked in figure 5.

Most of the ODCR data were taken with a wide slit setting and the spectrometer centred on the luminescence due to excitonic recombination. This eliminated changes in PL intensity due to the diamagnetic shift and provided ample luminescence signal. It did not differentiate between different luminescence transitions; a negative ODCR signal results from a net decrease of the total PL with FIR illumination. Comparison of the PL and IMPL traces, however, indicates how the FIR radiation impacts on the intensities of the differing PL transitions.

Figure 12 shows the PL and IMPL signals at the resonance field of the  $1s-2p_+$  transition for a FIR wavelength of  $163 \mu\text{m}$ . The intensity of the ( $D^0,X$ ), ( $D^+,X$ ) and ( $A^0,X$ ) complexes is sharply reduced when illuminated by the FIR. Attenuation of the PL intensity originating in this triplet of peaks often approached 50% under resonant conditions. An increase in PL intensity is observed for the free electron to acceptor transition, ( $e,A^0$ ), at longer wavelengths. The increase in PL intensity for this transition is contrary to the findings of Wright *et al* [2] in their ODCR study of bulk GaAs but agrees with a parallel study by Moll *et al* [4].

The IMPL spectrum in figure 12 illustrates the principal mechanism at work in optically detected cyclotron resonance: donor electrons, excited by the FIR from the ground  $1s$  level into higher impurity states, have an increased probability of being ejected into the conduction band by absorption of phonons [34]. A greater number of free electrons will suppress the formation of excitons and increase the impact ionization process whereby an electron knocks the remaining bound excitons off their donor sites. This results in a decrease of the PL due to bound excitons. There is a visible enhancement of the ( $e,A^0$ ) transition, signifying an increase in the number of conduction band electrons.

Support for this contention comes from photoconductivity measurements, where a current increase across



a sample is seen at field values corresponding to impurity transitions [35, 36]. A luminescence study monitoring the influence of  $10.6 \mu\text{m}$  radiation on edge luminescence in n-GaAs attributed quenching of transitions involving both donor and acceptor bound excitons to the liberation of electrons and holes from their respective impurity centres by the near-infrared radiation [37]. Additional evidence is provided by luminescence intensity measurements as a function of electric bias voltage [38], which showed similar changes in individual peak intensity to those observed in the present study and indicated that weakly bound excitons are first to be ionized when the field strength is increased.

As noted earlier, high energy impurity transitions continue to give a negative ODCR signal throughout the field range, while lower energy impurity transitions produce a positive ODCR signal above 8 T. We believe the cause for the changeover is twofold: Firstly, the magnetic field increases the magnitude of the  $(D^0, X)$  transition relative to the other excitonic transitions (cf figure 11). Changes to the  $(D^0, X)$  complex therefore influence the ODCR signal more heavily at higher fields. Secondly, the increase in field suppresses the photothermal ionization of carriers from lower lying impurity levels up to the conduction band. This has been shown in far-infrared photoresponse studies of high purity InP [39] and GaAs [40], where the application of field results in extremely long lifetimes of carriers confined in lower lying impurity states like the  $2p_-$ .

It is possible that carriers which are stuck in these 'bottleneck' states could lead to the formation of donor bound excitons directly in excited states. For example, a donor with its electron confined to the  $2p_-$  level would capture an exciton and result in a state that could be labelled  $(D_{2p_-}, X)$ . These excited donor bound excitons would provide the specific mechanism that results in the observed positive ODCR signals at higher field. The larger extent of the donor electron wavefunction when excited by the FIR into a higher impurity state would increase the donor capture cross section and subsequent probability of exciton capture. An increase in luminescence intensity with FIR radiation would then be expected at high fields when the photothermal effect is only weakly operative. Additionally, the 'Auger'-like process used to explain the temperature dependence of luminescence peak intensity [27] could also contribute to the changeover from negative to positive ODCR signal. Interactive processes like the Auger effect are usually confined to materials with extremely high carrier concentrations, but in the case of an exciton bound to a neutral donor the three required carriers are confined to the region surrounding the donor. The increasing size of the donor electron wavefunction with FIR illumination would also serve to weaken the overlap between the 'exciton hole' and 'donor electron'. The probability of the non-radiative 'Auger' process would be decreased, leading to more radiative recombination and thus more luminescence.

The presence of excited donor bound exciton states with FIR illumination might be expected to shift the

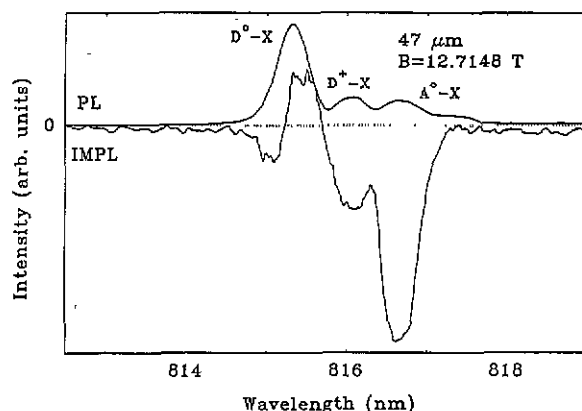


**Figure 13.** PL and IMPL traces for a FIR wavelength of  $47 \mu\text{m}$  taken at  $12.715 \text{ T}$ , which corresponds to the  $1s-2p_+$  transition. FIR radiation attenuates the  $(D^+-X)$  and  $(A^0-X)$  lines but has a differential effect on the  $(D^0-X)$  transition.

luminescence recombination energy slightly. The limit of maximum excitation of the donor electron to higher impurity states would be the  $(D^+, X)$  transition, where the exciton binds to a donor whose electron has been ionized. Evidence for excited donor bound exciton states would therefore occur in the portion of the  $(D^0, X)$  line that adjoins the  $(D^+, X)$  peak. Under FIR illumination the excited donor bound exciton states would be expected to increase their radiative recombination, while the standard donor bound exciton line might decrease slightly due to the weakened photothermal effect. This is exactly what we observe. Pictured in figure 13 are the PL and IMPL signals corresponding to the  $1s-2p_+$  resonance for  $47 \mu\text{m}$  at  $12.7 \text{ T}$ . For the  $(D^+, X)$  and  $(A^0, X)$  peaks there is a direct correspondence between the PL and IMPL trace. The IMPL signal for the  $(D^0, X)$  transition, however, shows a positive signal close to the  $(D^+, X)$  peak and a slightly negative signal at shorter wavelengths. An IMPL spectrum of the lower energy  $1s-2p_-$  resonance for  $251 \mu\text{m}$  (figure 14) reveals only a positive  $(D^0, X)$  contribution to the ODCR signal. This

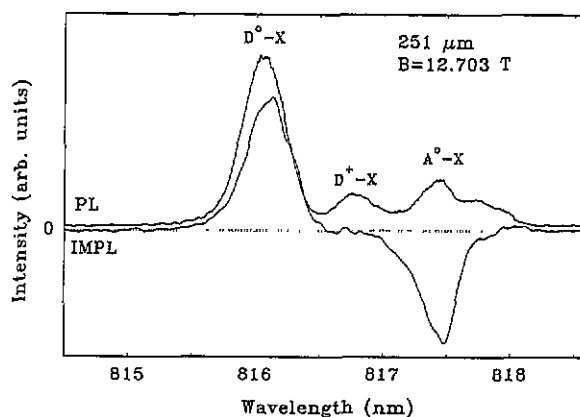


**Figure 14.** PL and IMPL traces for a FIR wavelength of  $251 \mu\text{m}$  taken at  $12.703 \text{ T}$ , which corresponds to the resonant position of the silicon impurity  $1s-2p_-$  transition. FIR radiation results in an enhancement of  $(D^0-X)$  intensity but reduces the radiative recombination of the  $(D^+-X)$  and  $(A^0-X)$  lines. An ODCR trace of this lower energy impurity resonance taken with wide slits would produce an overall positive signal.

again illustrates the role that lower lying donor states have in the process of excitonic recombination.

Differential-like IMPL signals have been previously observed in GaAs/AlGaAs quantum wells [5] and heterostructures [3, 41]. Ahmed *et al* ascribed the positive portion to resonant heating of free carriers, thereby increasing free exciton emission and decreasing ( $D^0, X$ ) emission. No increase in free exciton emission is observed in our data or in their bulk GaAs spectra [3], casting doubts on the validity of this hypothesis.

## 6. Conclusions

Optically detected cyclotron resonance has been performed on a high quality sample of bulk GaAs. Experimentally, ODCR is shown to be a viable experimental technique for free-electron mass determination and impurity studies. Transitions from the impurity ground state to excited states with hydrogen-like analogues are described well by the energy levels predicted by Makado and McGill. Chemical shifts to these impurity levels due to different donors in the sample are completely resolved at full field. Metastable states exist, appearing as broad resonances, and are fitted using an existing theory. The ODCR signal is shown to be primarily due to the photothermal effect, where larger numbers of electrons are freed by FIR illumination from donor sites into the conduction band. This increases the impact ionization of bound excitons and results in a decrease of luminescence intensity due to excitonic recombination and a corresponding increase in free-electron-related luminescence. At higher fields, a complex interaction between donor electrons and the donor bound exciton energy spectrum results in an enhancement of a portion of the ( $D^0, X$ ) PL transition.

## References

- [1] Romestain R and Weisbuch C 1980 *Phys. Rev. Lett.* **45** 2067
- [2] Wright M G, Ahmed N, Mitchell K, Koohian A, Pidgeon C R, Cavenett B C, Stanley C R and Kean A H 1990 *Semicond. Sci. Technol.* **5** 438
- [3] Ahmed N, Agoon I R, Wright M G, Mitchell K, Koohian A, Adams S J, Pidgeon C R, Cavenett B C, Stanley C R and Kean A H 1992 *Semicond. Sci. Technol.* **7** 352
- [4] Moll A, Wetzel C, Meyer B K, Omling P and Scholz F 1992 *Phys. Rev. B* **45** 1504
- [5] Warburton R J, Michels J G, Nicholas R J, Foxon C T and Harris J J 1992 *Phys. Rev. B* **46** 13394
- [6] Warburton R J, Michels J G, Peyla P, Nicholas R J, Foxon C T and Harris J J 1993 *Solid State Electron.* to be published
- [7] Makado P C and McGill N C 1986 *J. Phys. C: Solid State Phys.* **19** 873
- [8] von Klarenbosch A, Klassen T O, Wenckeback W Th and Foxon C T 1990 *J. Appl. Phys.* **67** 6323
- [9] Wagner H P and Prettl W 1988 *Solid State Commun.* **66** 367
- [10] Armistead C J, Stradling R A and Wasilewski Z 1989 *Semicond. Sci. Technol.* **4** 557
- [11] Grimes R T, Stanaway M B, Chamberlain J M, Henini M and Hughes O H 1989 *Semicond. Sci. Technol.* **4** 548
- [12] Simola J and Virtamo J 1978 *J. Phys. B: At. Mol. Phys.* **11** 3309
- [13] Simmonds P E, Chamberlain J M, Hoult R A, Stradling R A and Bradley C C 1974 *J. Phys. C: Solid State Phys.* **17** 4164
- [14] Stanley C R, Holland M C and Kean A H 1991 *Appl. Phys. Lett.* **58** 478
- [15] Hopkins M A, Nicholas R J, Pfeffer P, Zawadzki W, Gauthier D, Portal J C and DiForte-Poisson M A 1987 *Semicond. Sci. Technol.* **2** 568
- [16] Sigg H, Perenboom J A J, Pfeffer P and Zawadzki W 1987 *Solid State Commun.* **61** 685
- [17] Wasilewski Z and Stradling R A 1986 *Semicond. Sci. Technol.* **1** 264
- [18] Holmes S R *et al* 1989 *Semicond. Sci. Technol.* **4** 782
- [19] Hawksworth S J *et al* 1992 *Semicond. Sci. Technol.* **7** 1499
- [20] Grimes R T, Stanaway M B, Singleton K, Langerak C J G M, Chamberlain J M, Stanley C R and Cheng T 1991 *Gallium Arsenide and Related Compounds 1990 (Inst. Phys. Conf. Ser. 112)* ed K E Singer (Bristol: IOP Publishing) ch 4
- [21] Heim U and Hiesinger P 1974 *Phys. Status Solidi b* **66** 461
- [22] Bimberg D, Munzel H, Steckenborn A and Christen J 1985 *Phys. Rev. B* **31** 7788
- [23] Zemon S and Lambert G 1989 *Solid State Commun.* **70** 855
- [24] Hwang C J 1973 *Phys. Rev. B* **8** 646
- [25] Hopfield J J 1964 *Proc. 7th Int. Conf. on the Physics of Semiconductors* (Paris: Dunod) p 725
- [26] Tomaru T, Ohyama T and Otsuka E 1992 *Phys. Rev. B* **46** 9390
- [27] Bebb H B and Williams E W 1972 *Semiconductors and Semimetals 8* ed R K Willardson and A C Beer (New York: Academic) p 182
- [28] Hwang C J and Dawson L R 1972 *Solid State Commun.* **10** 443
- [29] Rorison J, Herbert D C, Dean P J and Skolnick M S 1984 *J. Phys. C: Solid State Phys.* **17** 6435
- [30] Dean P J and Skolnick M S 1983 *J. Appl. Phys.* **54** 346
- [31] Harris T D, Skolnick M S, Parsey J M Jr and Bhat R 1988 *Appl. Phys. Lett.* **52** 389
- [32] Driessen F A J M, Lochs H G M, Olsthoorn S M and Gilling L J 1991 *J. Appl. Phys.* **69** 906
- [33] Hickmott T W 1988 *Phys. Rev. B* **38** 12404
- [34] Sidorov V I and Lifshitz T M 1966 *Sov. Phys.-Solid State* **8** 2000
- [35] Kogan S M and Sedunov B I *Sov. Phys.-Solid State* (8)
- [36] Kurkova E A and Sidorov V I 1975 *Sov. Phys.-Semicond.* **9** 850
- [37] Akimov A V and Shofman V G 1991 *Sov. Phys.-Semicond.* **25** 961
- [38] Bludau W and Wagner E 1976 *Appl. Phys. Lett.* **29** 204
- [39] Chamberlain J M, Reeder A A, Claessen L M, Rikken G L and Wyder P 1987 *Phys. Rev. B* **35** 2391
- [40] Allan G R, Black A, Pidgeon C R, Gornik E, Seidenbusch W and Colter P 1985 *Phys. Rev. B* **31** 3560
- [41] Gubarv S I, Dremin A A, Kukushkin I V, Malyavkin A V and Tyazhlov M G 1991 *JETP Lett.* **54** 355